

Control strategy of PMSG based wind energy conversion system under strong wind conditions

Hidehito Matayoshi^{a,*}, Abdul Motin Howlader^b, Manoj Datta^c, Tomonobu Senju^a

^aUniversity of the Ryukyus, 1 Senbaru, Nishihara-cho, Nakagami, Okinawa 903-0213, Japan

^bUniversity of Hawaii, Manoa, Honolulu, Hawaii 96822, USA

^cRMIT University, 124 La Trobe Street, Melbourne, VIC 3000, Australia

ARTICLE INFO

Article history:

Received 24 November 2017

Received in revised form 13 April 2018

Accepted 9 July 2018

Available online xxx

MSC:
00-01
99-00

Keywords:

WECS
PMSG
Pitch angle control
Strong wind conditions

ABSTRACT

This paper presents a control approach for the Permanent Magnet Synchronous Generator (PMSG) based Wind Energy Conversion Systems (WECS) under a wide range of wind speeds. Generally, most of the wind turbines are turned-off and disconnected from the power grid, in case wind velocity is gone over 25 m/s. It may cause wind power supply shortage from wind farms. This research introduces a pitch angle controller as well as a rotational speed control system so that the PMSG based WECS can generate power if the wind speeds are above 25 m/s. The proposed method reduces the mechanical stress of the wind turbine by preferential reducing of the rotational speed rather than the mechanical torque during strong wind condition. As a result, the chance of turning-off the is reduced compared to the conventional control system because the PMSG based WECS can temporarily tolerate the wind speed up to 35 m/s. A 2 MW WECS with the electrical and mechanical characteristics is modeled in the MATLAB/SimPowerSystems[®] to verify the proposed research.

© 2017 Elsevier Inc. All rights reserved.

Introduction

Consumption of fossil fuels for generating electric power causes environmental pollutions and possible global warming (Cader, Bertheau, Blechinger, Huyskens, & Breyer, 2016). Alternatively, electric power generation by the nuclear power plants is risky due to the unreliable behavior of the plant and the possible challenges of nuclear waste dumping. Therefore, electric power generation using renewable energies are gaining huge momentum around the world (Kobayakawa & Kandpal, 2016; Oliver, Lew, Redlinger, & Prijyanonda, 2001). Common sources of renewable energies are wind power (Cooney, Byrne, Lyons, & O'Rourke, 2017), solar energy (dos Santos, Canha, & Bernardon, 2018), hydropower (Domenech, Ferrer-Martí, Lillo, Pastor, & Chiroque, 2014), bio-fuel (Shamsul, Kamarudin, & Rahman, 2017) and so on. Among them, WECS has the largest market share and is expected to maintain rapid growth in the coming years (Huang, Li, & Jin, 2015). Usually, WECS uses two types of wind turbines: Variable-Speed Wind Turbine (VSWT) (Chen & Song, 2016) and Fixed Speed Wind Turbine (FSWT) (Rodríguez-Amenedo, Arnaltes, & Rodríguez, 2008). The VSWTs have many advantages such

as Maximum Power Point Tracking (MPPT) during operation, better performance and control of the power output (Ajami, Alizadeh, & Elmi, 2016; Wei, Zhang, Qiao, & Qu, 2015). In recent years, the use of VSWTs with the PMSGs have been increased because of their higher efficiency, simpler structure and easy maintenance compared to the other generators (Yao, Liu, Zhou, Hu, & Chen, 2017). Generally, the AC-DC-AC power conversion system is utilized as the basic topology for the PMSG based WECS (Wei, Zhang, Qiao, & Qu, 2016). This kind of topology does not require synchronizing the rotational speed with the grid frequency. Also, the gearbox can be omitted for the directly driven operation of the PMSG (Yoon, He, & Hecke, 2015). Therefore, a PMSG based WECS with AC-DC-AC conversion circuit is a subject of research in this paper, specially its operation in the strong wind conditions.

Mechanical stress due to strong wind conditions is one of the operational challenges for WECS. Japan is a typhoon prone country, more specifically Okinawa prefecture of Japan faces one average 11 typhoons every year. When the wind speed exceeds 25 m/s, most wind turbines stop the power generation and are shut down (Aho et al., 2012; Giallanza, Porretto, Cannizzaro, & Marannano, 2017). It reduces energy utilization efficiency of the WECS. In addition, shutting down of the large wind turbine or wind farm causes severe frequency fluctuations which may lead to the power system instability and a cascaded failure. In Yuan and Tang (2017), an adaptive control

* Corresponding author.

E-mail address: e115526@yahoo.co.jp (H. Matayoshi).

strategy is proposed for reducing extreme loads and fatigues of the wind turbine when operated under high wind speeds. However, as the wind turbine is operated at the rated speed in the high wind conditions, it could be a matter of safety concern. As the cause of main mechanical stress is centrifugal force rather than the wind pressure, unexpected rise in the rotational speed warrants a serious caution. An Artificial Neural Network (ANN) based pitch angle control is developed in Dahbi, Nait-Said, and Nait-Said (2016). It can operate in the wide range of wind speed, however; mechanical stress at the high wind speeds is not considered in the development of the pitch angle controller.

Considering the research gaps of Yuan and Tang (2017) and Dahbi et al. (2016), a novel control strategy for the PMSG based WECS is presented in this paper. The novelty lies within the consideration that the proposed control strategy reduced mechanical loads the wind turbine by a preferential reduction of the rotation speeds and not by reducing the mechanical torque during strong wind conditions. In the proposed method, the PMSG based WECS can temporarily tolerate wind speed up to 35 m/s. As a result, the WECS can generate power during strong wind conditions which is important for a typhoon prone area like Okinawa. Performance of the proposed control system is verified via numerical simulation results obtained in the MATLAB/SimPowerSyems® environment.

The paper is organized as follows: in *Wind energy conversion system*, the mathematical model of WECS used for the simulation is developed. The conventional control and the proposed control are described in *Control strategy for power generation*. In *Configuration of the control systems*, control strategies for AC-DC-AC conversion systems and pitch angle are presented in detail. Simulation results and discussions shows the simulation results and discusses the performances of the WECS with a comparison of the conventional control and the proposed control. Finally, a summary of the discussions is presented in *Conclusion*.

Wind energy conversion system

A generic single line diagram of a PMSG based WECS is shown in Fig. 1. Wind energy is converted to variable frequency electric power by the PMSG. This power is supplied to the grid after converting it to a fixed frequency electric power via the AC-DC-AC conversion systems which comprises of a Machine-Side Converter (MSC) and a Grid Side Converter (GSC) connected by a DC-link capacitor. The GSC controls the rotational speed, as well as the output power of the PMSG. The system after the DC link is modeled as a voltage source because the system is the same as a conventional system.

Wind turbine model

Fig. 2 shows the wind turbine and the PMSG models. The wind turbine converts wind energy to mechanical power P_w . The mechanical power P_w extracted from the wind is expressed as:

$$P_w = \frac{1}{2} C_p(\lambda, \beta) \rho \pi R^2 V_w^3 \quad (1)$$

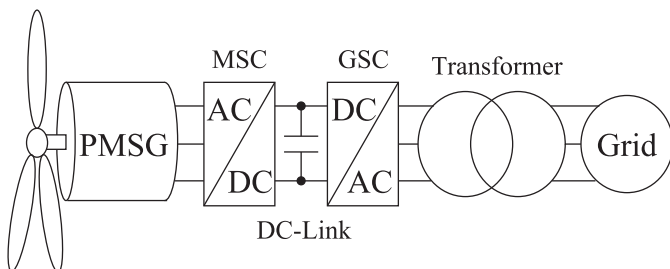


Fig. 1. Block diagram of a variable speed PMSG based WECS.

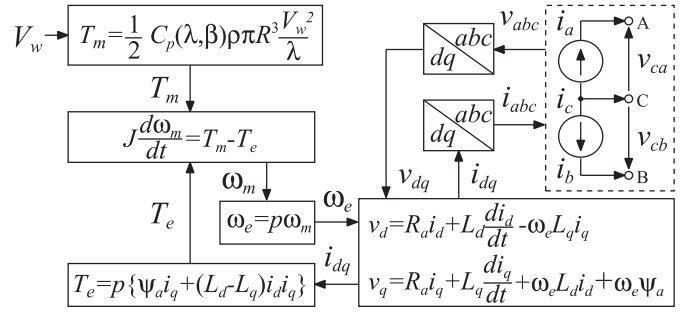


Fig. 2. Block diagrams of the wind turbine and PMSG models.

where C_p is the power coefficient of the wind turbine, $\lambda = \omega_m R / V_w$ is the tip speed ratio, ω_m is the wind turbine mechanical rotational speed, β is the pitch angle, ρ is the air density, R is the radius of the wind turbine blades and V_w is the wind velocity. The wind turbine input mechanical torque T_m is given by:

$$T_m = \frac{1}{2} C_p(\lambda, \beta) \rho \pi R^3 \frac{V_w^2}{\lambda} \quad (2)$$

and the power coefficient of wind turbine C_p is given by the following equations (Yin, Li, Zhou, & Zhao, 2007):

$$C_p = 0.22 \left(\frac{116}{\lambda_i} - 0.4\beta - 5 \right) \exp \frac{-12.5}{\lambda_i} \quad (3)$$

$$\lambda_i = \frac{1}{\frac{1}{\lambda + 0.08\beta} - \frac{0.035}{\beta^3 + 1}} \quad (4)$$

PMSG model

The mathematical model of a PMSG is the same as the Permanent Magnet Synchronous Motor (PMSM). PMSG is modeled in the synchronous d-q frames by the following voltage and electrical torque equations (Uehara et al., 2011):

$$v_d = R_a i_d + L_d \frac{di_d}{dt} - \omega_e L_q i_q \quad (5)$$

$$v_q = \omega_e L_d i_d + R_a i_q + L_q \frac{di_q}{dt} + \omega_e K \quad (6)$$

$$T_e = p \{ K i_q + (L_d - L_q) i_d i_q \} \quad (7)$$

where v_d is the d-axis voltage and v_q is the q-axis voltage, i_d is the d-axis current and i_q is the q-axis current, R_a is the stator resistance, L_d is the d-axis inductance and L_q is the q-axis inductance, ω_e is the electrical rotational speed, K is the magnetic flux, and p is the number of pole pairs. The motion equation is expressed as the following (Uehara et al., 2011):

$$J \frac{d\omega_e}{dt} = T_m - T_e \quad (8)$$

where J is the inertia.

Control strategy for power generation

Fig. 3 shows a typical WECS output power curve for the conventional and proposed controls with respect to the pitch angle. First,

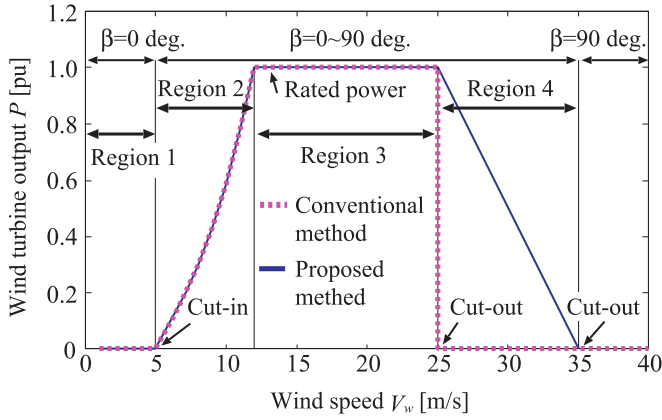


Fig. 3. Output power control strategy.

the conventional control strategy is described. The dotted line on Fig. 3 indicates the conventional control strategy. When the wind velocity is between 5 and 12 m/s, MPPT control is utilized for the WECS to generate maximum power. The MPPT control is performed by controlling the rotational speed due to adjusting the duty ratio of the MSC as well as the generator currents. The pitch angle control is activated so that the output power remains constant at the rated power when the wind velocity is between 12 and 25 m/s. If the wind velocity reaches 25 m/s, the wind generator is turned-off, and the pitch angle is set to 90°. In general, if the averaged wind velocity over 10 min is more than 25 m/s or the averaged wind velocity averaged over 3 s is more than 30 m/s, the wind generation is forced to switch-off.

Next, the proposed control strategy is described. Fig. 3 indicates the proposed control strategy for power generation as a solid line. Moreover, the wind speed ranges are shown as Regions 1, 2, 3, and 4. In Region 2, the proposed control method is same as the conventional method. In Region 3, not only the pitch angle control but also rotational speed control are adopted for the WECS. The hybrid control enables high-precision output control. The proposed method can ensure safety in strong wind conditions because it decreases the rotation speed as the wind speed increases. The main stresses on the wind turbine are aerodynamic loads on the blade and centrifugal force. Particularly, the centrifugal force is a product of rotational velocity squared and mass, which always acts radial outward, hence the raised load demands of higher tip speeds (Shokrieh & Rafiee, 2006). Therefore, the proposed method preferentially reduces

the rotational speed rather than the mechanical torque during the strong wind condition. As a result, the allowable condition of power generation can temporarily reach up to the wind speed from 25 m/s to 35 m/s in Region 4 because the proposed control significantly reduces the power coefficient and the centrifugal force. In other words, the power generation is continued until the averaged wind velocity over 10 min exceeds 30 m/s or the averaged wind velocity over 3 s exceeds 35 m/s which helps to improve the overall efficiency of the PMSG based WECS.

Configuration of the control systems

Fig. 4 illustrates the MSC control system. The MSC is comprised of six Insulated Gate Bipolar Transistors (IGBT) which are switched ON/OFF by using the triangular-wave PWM method. The control is based on the measurements of wind speed, generator voltages, currents, and rotational speed. Although, wind speed measurement in WECS control is not recommended (Tiwari, Padmanaban, & Neelakandan, 2017). However, appropriate output power is defined based on the measured wind speed in this research. This is because determination of the operating area is important to ensure safety in the strong wind condition. Naturally, typical wind speed estimation can be also applied to the system as in Bonfiglio, Delfino, Invernizzi, & Procopio, 2017. An anemometer is used for simplicity in this paper. The details of both control systems are described in the following subsections.

Rotational speed and torque control system

The rotational speed and torque control systems are shown in Fig. 4. The error between the reference rotational speed and measured rotational speed is processed through a PI controller. The controller generates the q -axis reference current i_q^* . Output power characteristics of the WECS are depicted in Fig. 5. Dots represent maximum power points for the discrete steps in wind speed. Each power curve contains the optimal rotational speed ω_{opt} corresponds to maximum wind power generation. In MPPT control area (Region 2), the pitch angle β is set to 2°. Here, the optimal rotational speed ω_{opt} is represented by optimal tip speed ratio λ_{opt} and wind velocity V_w as follows:

$$\omega_{opt} = \lambda_{opt} V_w. \tag{9}$$

If the rotational speed ω_m is equal to the optimal rotational speed ω_{opt} , the output power will be maximum.

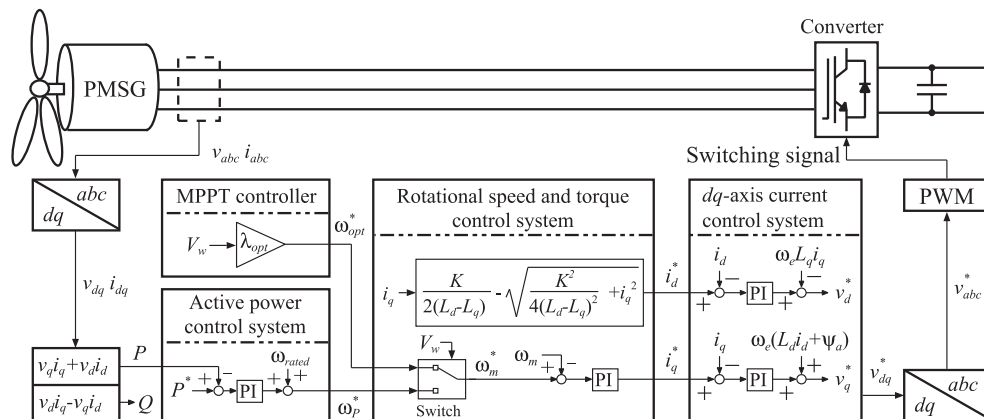


Fig. 4. Configuration of proposed converter control system.

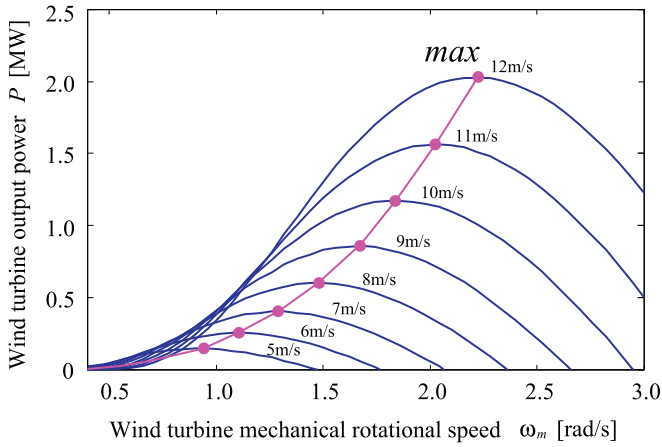


Fig. 5. Wind turbine output power characteristics.

In this paper, a salient-pole type PMSG is used. In order to achieve the maximum torque from the PMSG, the d -axis reference current i_d^* is determined by the following equation (Uehara et al., 2011):

$$i_d^* = \frac{K}{2(L_d - L_q)} - \sqrt{\frac{K^2}{4(L_d - L_q)^2} + i_q^2} \quad (10)$$

Active power control system

The active power control system is shown in Fig. 4. The reference rotational speed ω_m^* is the sum of the rated rotational speed ω_{rated} and the output of the PI based power controller. This output is a correction value to compensate the performance of the power tracking reference. The controller is used for the rated power control (Region 3) and power suppression control (Region 4). In Region 3, the reference power P^* is equal to the rated power P_{rated} . In Region 4, the output command value is decreased linearly according to the increase in the wind speed. A sudden disconnection from the power system is prevented and the operating region of the wind speed is considered up to 35 m/s.

dq-Axis current control system

The dq-axis current control system is shown in Fig. 4. This a decoupling based synchronous frame PI controller where the d -axis and q -axis current errors are processed through the respective PI controllers. Then decoupling terms are added or subtracted to produce d -axis and q -axis reference voltages v_{dq}^* .

Pitch angle control system

The pitch angle control is applied for Regions 3 and 4 as it needed for the output power control. The conventional pitch angle control system is shown in Fig. 6. In this method, the output power

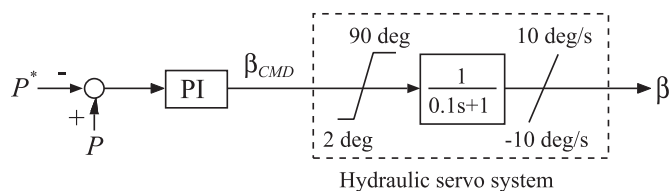


Fig. 6. Conventional pitch angle control system.

of the PMSG is controlled by using only the pitch angle control system. The pitch angle command value β_{CMD} is obtained from the PI controller. Input of the PI controller is the deviation between the power command value P^* and the measured output power P . The output power command value P^* is set as the rated power P_{rated} (2 MW) in Region 3. The operating mechanism of the pitch angle control is realized by a hydraulic servo system. The hydraulic servo system has 0.1 s time lag and the operating speed of the pitch angle control is $\pm 10^\circ/s$. The tracking speed and accuracy of the conventional pitch angle control are not so good as the pitch changing speed is slow. The proposed pitch angle controller will try to improve the performance.

The proposed pitch angle control system is shown in Fig. 7. In this method, reference pitch is correlated with wind speed rather than the power. The pitch angle reference β^* in the Regions 3 and 4 is determined by a lookup table as shown in Fig. 8. The pitch angle reference is designed so that it makes the rotational speed lower than the rated rotational speed. When the wind speed is more than 25 m/s, the rotational speed is sufficiently reduced. However, excessive reduction in rotational speed requires small pitch angles and excessive mechanical torques. Hence, the balance of stresses due to centrifugal force and mechanical torque are regulated by the proposed pitch angle reference.

Simulation results and discussions

In this section, the conventional and proposed methods are compared based on same conditions. Note that the same conditions mean that the wind velocity, PMSG parameters, wind turbine parameters and parameters of PI controller are same in both models. These parameters of PI controller are chosen by empirical knowledge. Table 1 shows the parameters of the wind turbine and PMSG. In Operation of wind turbine under a linear wind velocity, conventional and proposed methods are compared under a linear wind velocity with small oscillations as shown in Fig. 9a and the simulation results are shown for all the operating regions. In Operation of wind turbine under a wind velocity when a typhoon is landed, these two methods are compared under a wind velocity when the typhoon is landed as shown in Fig. 9b. Therefore, the realistic behavior of wind turbines is demonstrated.

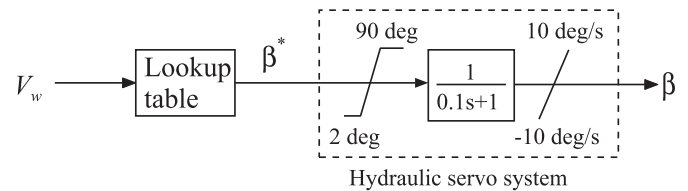


Fig. 7. Proposed pitch angle control system.

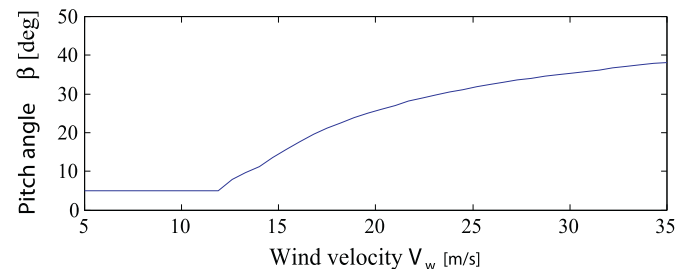


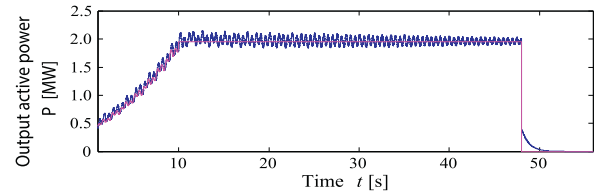
Fig. 8. Proposed pitch angle reference.

Table 1
Simulation parameters.

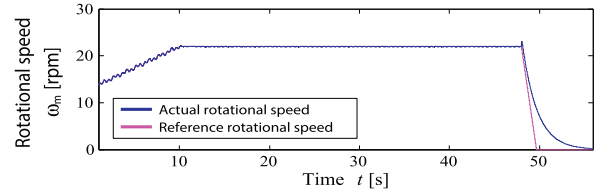
Parameters of wind turbine	
Blade radius R	38 m
Air density ρ	1.205 kg/m ³
Rated wind speed V_{w_rated}	12 m/s
Optimal tip speed ratio λ_{opt}	0.187
Parameters of PMSG	
Rated output P_{rated}	2 MW
Resistance R_d	50 $\mu\Omega$
d axis inductance L_d	5.5 mH
q axis inductance L_q	3.75 mH
Number of pole pairs p	11
Field flux K	136.25 V · s/rad
Inertia J	10,000 kg · m ²

Operation of wind turbine under a linear wind velocity

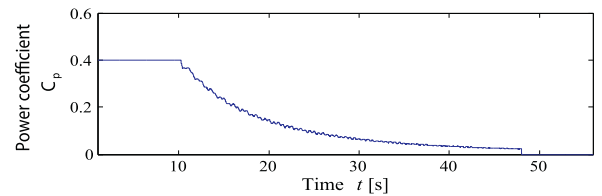
Figs. 10 and 11 illustrate the simulation results of the conventional and proposed methods, respectively. The wind speed increases from 8 to 35 m/s as shown in Fig. 9a. Therefore, it satisfies all the operating regions of WECSs. The generated power of the WECS is shown in Figs. 10a and 11a. In Region 2, both models perform the MPPT control. In Region 3, the output power with the conventional system follows the reference with oscillations because it is controlled by only pitch angle control. However, the output power with the proposed control exactly follows its reference. This is due to the employment of not only pitch angle control but also rotational speed control. In Region 4, the generated power with the conventional system is suddenly dropped when wind velocity exceeds 25 m/s. On the other hand, the generated power with the proposed system is suppressed to less than the rated power and generation is continued. The rotational speed of the wind turbine is shown in Figs. 10b and 11b. In Region 2, both mechanical rotational speeds are same because the same MPPT control is applied. In Region 3, the mechanical rotational speed with the conventional method is constant. Conversely, the proposed method controls the rotational speed to accurately adjust the generated power. Furthermore, it can ensure safety because the rotation speed is decreased in strong wind conditions to suppress



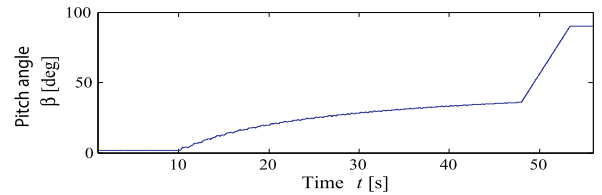
(a) Generated power of the WECS.



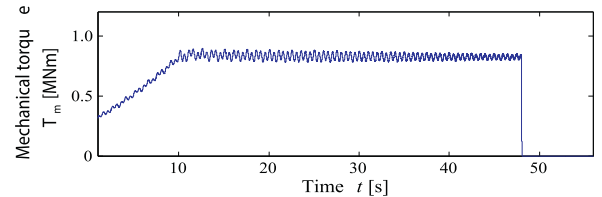
(b) Mechanical rotational speed.



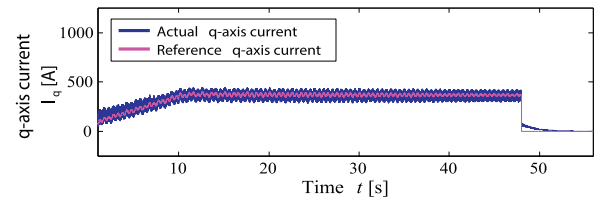
(c) Power coefficient.



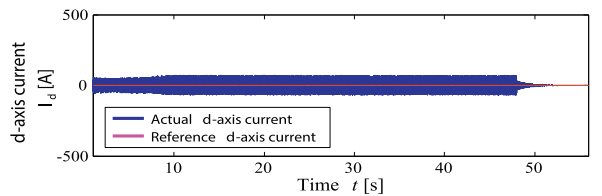
(d) Pitch angle.



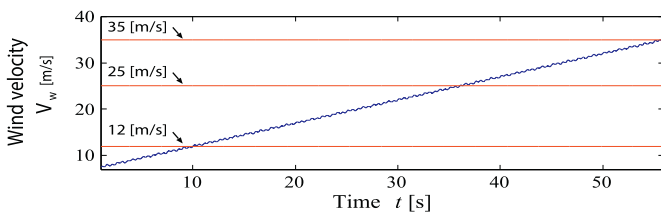
(e) Mechanical torque.



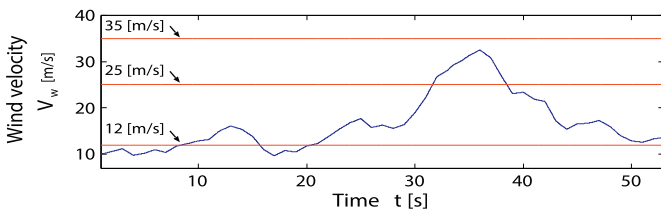
(f) q-axis current.



(g) d-axis current.



(a) Linear wind velocity with small oscillations.



(b) wind velocity when a typhoon is landed.

Fig. 9. Simulation results of the conventional method.

Fig. 10. Simulation results of the conventional method.

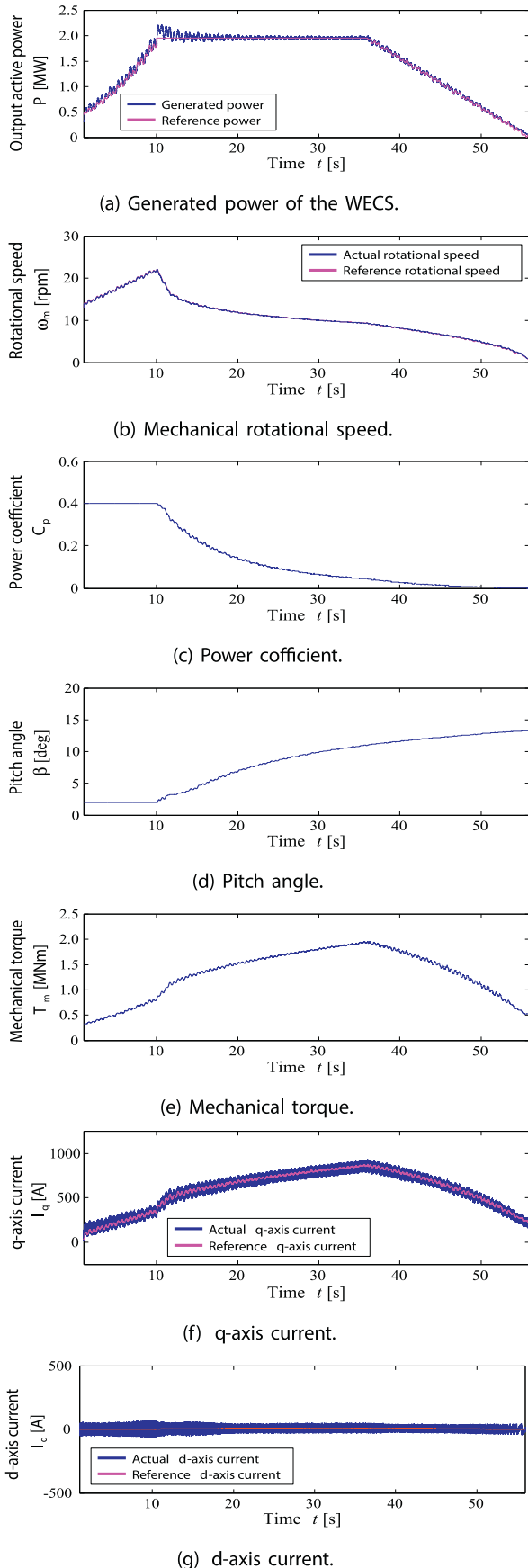


Fig. 11. Simulation results of the proposed method.

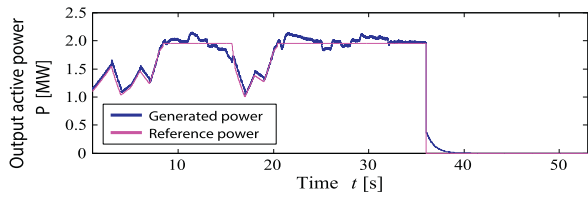
mechanical stress. The power coefficient is shown in Figs. 10c and 11c. In Region 2, the power coefficient is the maximum to achieve the MPPT control. In Region 3, it decreases according to the wind speed variation to maintain the rated power. In Region 4, the power coefficient becomes zero with the conventional control because the generation is stopped. However, the power coefficient does not drop to zero with the proposed control method. It indicates the continuation of the electricity generation. Figs. 10d and 11d show the pitch angle of the WECS. In the conventional method, the pitch angle is controlled by the PI controller in Region 3. In this method, the output power is fluctuated to up and down due to the presence of mechanical constraints. Then, the pitch angle becomes 90° with the conventional method after stopping of the wind turbine. On the other hand, the output power is stabilized due to using estimated optimum pitch angle in the proposed method. The mechanical torque changes along with the output power and the rotational speed as shown in Figs. 10e and 11e. Figs. 10f, 11f, 10g, and 11g show the q -axis and the d -axis currents. The control performance of these currents is similar for the conventional and proposed methods due to same dq -axis current control systems. From these simulation results, it can be confirmed that the power generation can be continued when wind speed exceeds 25 m/s by applying the proposed method.

Operation of wind turbine under a wind velocity when a typhoon is landed

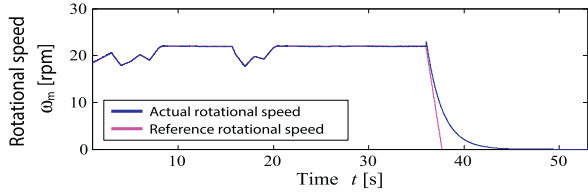
Fig. 9b shows the wind velocity that assumed a typhoon. The instantaneous wind velocity exceeds 30 m/s. Figs. 12 and 13 illustrate the simulation results of the conventional and proposed methods, respectively. The generated power of the WECS is shown in Figs. 12a and 13a. The wind turbine with the conventional method is stopped because the average wind velocity exceeds 30 m/s. However, with the proposed method the power generation continues even when strong wind occurs. The rotational speed of the wind turbine is shown in Figs. 12b and 13b. It can be confirmed that the rotor is stopped with the conventional method but the proposed control system allows continuation of rotation with a low speed. Figs. 12c and 13c illustrate the power coefficient. It can be seen that MPPT control is performed when the wind velocity is lower than 10 m/s. Further, the power coefficient is reduced when the wind speed is more than the rated wind velocity. Figs. 12d and 13d show the pitch angle of the wind turbine. In the conventional method, the pitch angle control is delayed due to a presence of mechanical constraints. Therefore, the output power has fluctuated. On the other hand, the output power is stabilized with the estimated optimum pitch angle in the proposed method. The mechanical torque changes along with the output power and rotational speed are shown in Figs. 12e and 13e. Figs. 12f, 13f, 12g, and 13g show the q -axis and the d -axis currents, respectively. The system for controlling these currents is same in both methods. From the simulation results, it can be said that the proposed method can generate power in strong wind conditions. Therefore, the proposed system increases the power efficiency.

Conclusion

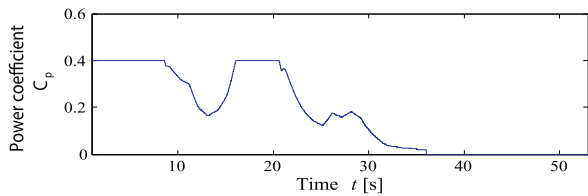
This paper describes a control method for the PMSG based WECS under strong wind conditions. Conventional control method is compared with the proposed control method considering same conditions and system parameters. In the MPPT control area, both conventional and proposed systems have shown similar performances. When the wind turbine is controlled at the rated power, the power fluctuation occurs with the conventional method. This is because, it is controlled by only the pitch angle control system with some delays. In the proposed method, both pitch angle and rotational speed control methods are designed for the wide-wind-range of wind velocity. As a result, the output power is controlled



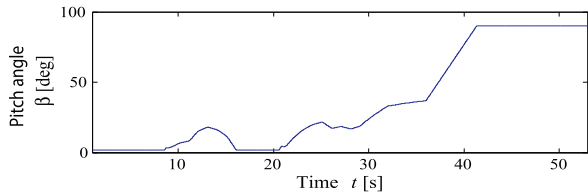
(a) Generated power of the WECS.



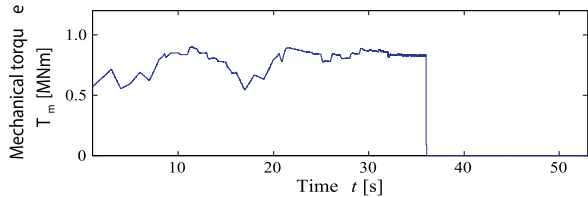
(b) Mechanical rotational speed.



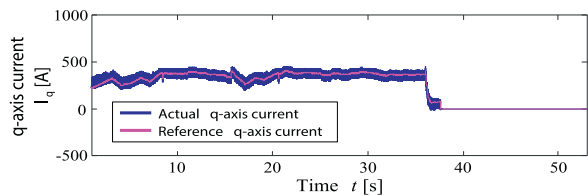
(c) Power coefficient.



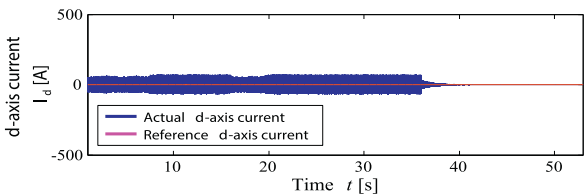
(d) Pitch angle.



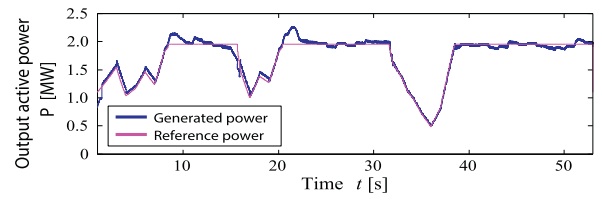
(e) Mechanical torque.



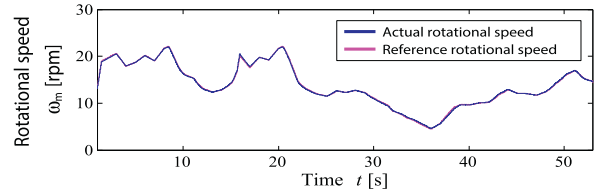
(f) q-axis current.



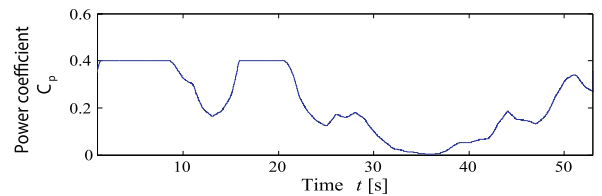
(g) d-axis current.



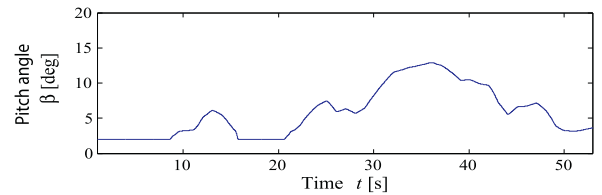
(a) Generated power of the WECS.



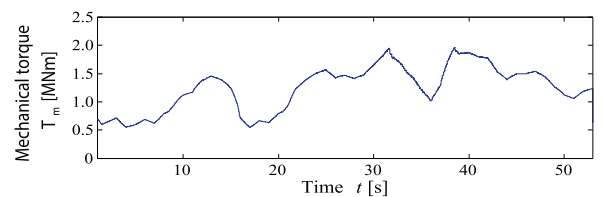
(b) Mechanical rotational speed.



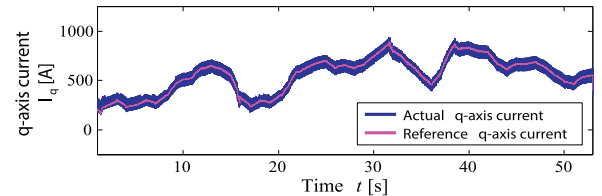
(c) Power coefficient.



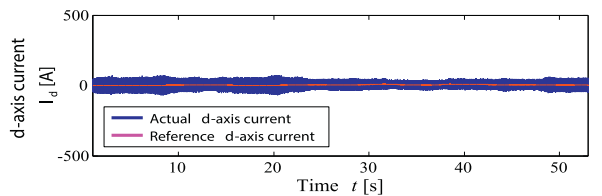
(d) Pitch angle.



(e) Mechanical torque.



(f) q-axis current.



(g) d-axis current.

Fig. 12. Simulation results of the conventional method.

Fig. 13. Simulation results of the proposed method.

with high accuracy by using the proposed method. In addition, the proposed method preferentially reduces the rotational speed rather than the mechanical torque in order to reduce the power coefficient and the centrifugal force during the strong wind conditions. For this reason, the allowable condition of power generation can temporarily reach up to the wind speed of 35 m/s. Therefore, it can be said that the PMSG based WECS with the proposed control method can avoid a sudden cut-off from the power grid during strong wind conditions as well as can continue to generate power in the typhoon prone area. However, if the wind speed goes above the 35 m/s the wind turbine needs to be shut down. In doing so it will give some time to bring appropriate load-frequency control action rather than sudden generation curtailment.

References

- Aho, J., Buckspan, A., Laks, J., Fleming, P., Jeong, Y., Dunne, F., ... Johnson, K. (2012). A tutorial of wind turbine control for supporting grid frequency through active power control. *2012 American Control Conference (ACC)*. (pp. 3120–3131). <https://doi.org/10.1109/ACC.2012.6315180>.
- Ajami, A., Alizadeh, R., & Elmi, M. (2016). Design and control of a grid tied 6-switch converter for two independent low power wind energy resources based on pmsgs with mppt capability. *Renewable Energy*, *87*(Part 1), 532–543. <https://doi.org/10.1016/j.renene.2015.10.031>.
- Bonfiglio, A., Delfino, F., Invernizzi, M., & Procopio, R. (2017). Modeling and maximum power point tracking control of wind generating units equipped with permanent magnet synchronous generators in presence of losses. *Energies*, *10*(1), <https://doi.org/10.3390/en10010102>.
- Cader, C., Bertheau, P., Blechinger, P., Huyskens, H., & Breyer, C. (2016). Global cost advantages of autonomous solar-battery-diesel systems compared to diesel-only systems. *Energy for Sustainable Development*, *31*(Supplement C), 14–23. <https://doi.org/10.1016/j.esd.2015.12.007>.
- Chen, J., & Song, Y. (2016). Dynamic loads of variable-speed wind energy conversion system. *IEEE Transactions on Industrial Electronics*, *63*(1), 178–188. <https://doi.org/10.1109/TIE.2015.2464181>.
- Cooney, C., Byrne, R., Lyons, W., & O'Rourke, F. (2017). Performance characterisation of a commercial-scale wind turbine operating in an urban environment, using real data. *Energy for Sustainable Development*, *36*(Supplement C), 44–54. <https://doi.org/10.1016/j.esd.2016.11.001>.
- Dahbi, A., Nait-Said, N., & Nait-Said, M.-S. (2016). A novel combined mppt-pitch angle control for wide range variable speed wind turbine based on neural network. *International Journal of Hydrogen Energy*, *41*(22), 9427–9442. <http://www.sciencedirect.com/science/article/pii/S0360319916303172>. <https://doi.org/10.1016/j.ijhydene.2016.03.105>.
- Domenech, B., Ferrer-Martí, L., Lillo, P., Pastor, R., & Chiroque, J. (2014). A community electrification project: Combination of microgrids and household systems fed by wind, pv or micro-hydro energies according to micro-scale resource evaluation and social constraints. *Energy for Sustainable Development*, *23*(Supplement C), 275–285. <https://doi.org/10.1016/j.esd.2014.09.007>.
- dos Santos, L., Canha, L., & Bernardon, D. (2018). Projection of the diffusion of photovoltaic systems in residential low voltage consumers. *Renewable Energy*, *116*(Part A), 384–401. <https://doi.org/10.1016/j.renene.2017.09.088>.
- Giallanza, A., Porretto, M., Cannizzaro, L., & Marannano, G. (2017). Analysis of the maximization of wind turbine energy yield using a continuously variable transmission system. *Renewable Energy*, *102*(Part B), 481–486. <https://doi.org/10.1016/j.renene.2016.10.067>.
- Huang, C., Li, F., & Jin, Z. (2015). Maximum power point tracking strategy for large-scale wind generation systems considering wind turbine dynamics. *IEEE Transactions on Industrial Electronics*, *62*(4), 2530–2539. <https://doi.org/10.1109/TIE.2015.2395384>.
- Kobayakawa, T., & Kandpal, T. C. (2016). Optimal resource integration in a decentralized renewable energy system: Assessment of the existing system and simulation for its expansion. *Energy for Sustainable Development*, *34*(Supplement C), 20–29. <https://doi.org/10.1016/j.esd.2016.06.006>.
- Oliver, T., Lew, D., Redlinger, R., & Priyanonda, C. (2001). Global energy efficiency and renewable energy policy options and initiatives. *Energy for Sustainable Development*, *5*(2), 15–25. [https://doi.org/10.1016/S0973-0826\(08\)60266-5](https://doi.org/10.1016/S0973-0826(08)60266-5).
- Rodríguez-Amenedo, J., Arnaltes, S., & Rodríguez, M. (2008). Operation and coordinated control of fixed and variable speed wind farms. *Renewable Energy*, *33*(3), 406–414. <https://doi.org/10.1016/j.renene.2007.03.003>.
- Shamsul, N., Kamarudin, S., & Rahman, N. (2017). Conversion of bio-oil to bio gasoline via pyrolysis and hydrothermal: A review. *Renewable and Sustainable Energy Reviews*, *80*(Supplement C), 538–549. <https://doi.org/10.1016/j.rser.2017.05.245>.
- Shokrieh, M. M., & Rafiee, R. (2006). Simulation of fatigue failure in a full composite wind turbine blade. *Composite Structures*, *74*(3), 332–342. <https://doi.org/10.1016/j.compstruct.2005.04.027>.
- Tiwari, R., Padmanaban, S., & Neelakandan, R.B. (2017). Coordinated control strategies for a permanent magnet synchronous generator based wind energy conversion system. *Energies*, *10*(10), <https://doi.org/10.3390/en10101493>.
- Uehara, A., Prata, A., Goya, T., Senjyu, T., Yona, A., Urasaki, N., & Funabashi, T. (2011). A coordinated control method to smooth wind power fluctuations of a PMSG-based WECS. *IEEE Transactions on Energy Conversion*, *26*(2), 550–558. <https://doi.org/10.1109/TEC.2011.2107912>.
- Wei, C., Zhang, Z., Qiao, W., & Qu, L. (2015). Reinforcement-learning-based intelligent maximum power point tracking control for wind energy conversion systems. *IEEE Transactions on Industrial Electronics*, *62*(10), 6360–6370. <https://doi.org/10.1109/TIE.2015.2420792>.
- Wei, C., Zhang, Z., Qiao, W., & Qu, L. (2016). An adaptive network-based reinforcement learning method for mppt control of pmsg wind energy conversion systems. *IEEE Transactions on Power Electronics*, *31*(11), 7837–7848. <https://doi.org/10.1109/TPEL.2016.2514370>.
- Yao, J., Liu, R., Zhou, T., Hu, W., & Chen, Z. (2017). Coordinated control strategy for hybrid wind farms with dfig-based and pmsg-based wind farms during network unbalance. *Renewable Energy*, *105*(Supplement C), 748–763. <https://doi.org/10.1016/j.renene.2016.12.097>.
- Yin, M., Li, G., Zhou, M., & Zhao, C. (2007). Modeling of the wind turbine with a permanent magnet synchronous generator for integration. *2007 IEEE Power Engineering Society General Meeting*. (pp. 1–6). <https://doi.org/10.1109/PES.2007.385982>.
- Yoon, J., He, D., & Hecke, B. V. (2015). On the use of a single piezoelectric strain sensor for wind turbine planetary gearbox fault diagnosis. *IEEE Transactions on Industrial Electronics*, *62*(10), 6585–6593. <https://doi.org/10.1109/TIE.2015.2442216>.
- Yuan, Y., & Tang, J. (2017). Adaptive pitch control of wind turbine for load mitigation under structural uncertainties. *Renewable Energy*, *105*, 483–494. <https://doi.org/10.1016/j.renene.2016.12.068>.